

Original Paper

Simple yet Effective Video-Based Epileptic Tonic-Clonic Seizure Detection

Yoshinao Yazaki¹, Satsuki Watanabe² and Yuichi Tanaka^{3*}

¹*Graduate School of BASE, Tokyo University of Agriculture and Technology, Japan*

²*Department of Psychiatry, Saitama Medical University Hospital, Japan*

³*Graduate School of Engineering, Osaka University, Japan*

ABSTRACT

Epilepsy, a prevalent neurological disorder, often leads to tonic-clonic seizures characterized by loss of consciousness and uncontrolled motor activity. Prompt detection of these seizures is crucial for effective nursing and diagnosis. This paper introduces a novel epileptic seizure detection method leveraging low-complexity video analysis, eliminating the need for body attachments or special equipment like markers or specific clothing. Our approach is straightforward: each video frame is segmented into blocks, and the average values of these blocks are computed. We then analyze the temporal changes in these averages using spectrograms. Our findings indicate that during tonic-clonic seizures, dominant frequency components typically range from 1 to 6 Hz and decrease as the seizure progresses. By capitalizing on these clinical observations, we have formulated effective detection rules. Experimental evaluations reveal that our method not only accurately detects epileptic seizures but also operates approximately four times faster than real-time on standard desktop computers. This efficiency and

*Corresponding author: Yuichi Tanaka, ytanaka@comm.eng.osaka-u.ac.jp. This work was supported in part by JSPS KAKENHI under Grant 22K12912.

accuracy underscore the potential of our method as a practical tool in epilepsy monitoring and management.

Keywords: Epilepsy, tonic-clonic seizure, video analysis, image processing, and image feature extraction.

1 Introduction

Epilepsy, a chronic neurological disorder affecting approximately 65 million people worldwide [30], is characterized by abnormal excessive neuronal activity in the brain, leading to sudden epileptic seizures. These seizures, particularly affecting motor function, necessitate continuous monitoring due to the unpredictability of their occurrence. However, constant caregiver surveillance poses significant challenges, underscoring the need for automated seizure detection systems to improve the quality of life (QOL) for patients, caregivers, and medical professionals.

The predominant seizure detection methods involve electroencephalogram (EEG) analysis [1, 2, 7, 12, 21, 28], mainly because epilepsy diagnosis often relies on long-term video-EEG monitoring in hospitals. However, EEG monitoring requires specialized equipment and expertise, making it impractical for long-term use outside hospital settings. Additionally, the necessary contact sensors for EEG are often uncomfortable for patients.

To address these limitations, various non-EEG epileptic seizure detection methods have been explored, including heart rhythm analysis [9, 23, 31], electromyography [10, 19, 29], and accelerometers [8, 18, 24, 27]. Nevertheless, most of these approaches still rely on contact sensors and require expert handling.

Video surveillance offers a promising contact-free alternative. This method can be categorized into marker-based (e.g., infrared reflectors [20], customized color pajamas [22]) and marker-free approaches. While marker-based methods suffer from similar drawbacks as contact sensors, marker-free methods, such as those using optical flow [11, 14–17], offer non-invasive, non-contact solutions. However, these methods generally incur high computational costs, limiting their application in low-power devices.

An alternative marker-free approach [15–17] analyzes pixel variations in video frames to detect clonic seizures in newborns. While computationally efficient, it falls short in detection accuracy compared to optical flow-based methods.

In response to these challenges, this paper introduces a novel, efficient method for video-based epileptic seizure detection, specifically targeting clonic seizures in tonic-clonic episodes. Our approach utilizes spectrogram analysis

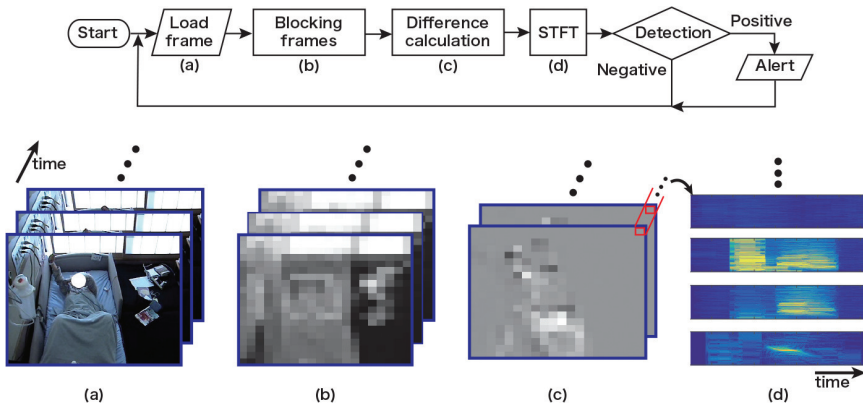


Figure 1: Flow of the proposed method. The top figure is a flow of the proposed method and the bottom figures are examples of the output of each step. The patient’s face is masked in this figure for anonymity. This is not part of the proposed method.

through short-time Fourier transform (STFT) to track body pixel value oscillations during seizures. The crux of our method lies in a detection rule based on a clinical observation: during clonic seizures, the frequency components of body oscillations show high magnitudes within a specific range, with dominant frequencies decreasing over time. The method’s workflow is depicted in Figure 1. We validated our approach’s detection accuracy through experiments with videos from long-term video EEG monitoring, highlighting its potential as a practical, efficient tool for epilepsy management.

The remainder of this paper is organized as follows. Section 2 introduces related work to this paper. In Section 3, video acquisition and the proposed method are described. Section 4 describes the experimental verification of the proposed method for detection accuracy and computation time, and we discuss the experimental results. Finally, Section 5 concludes this paper.

2 Related Work

The field of video-based seizure detection has evolved significantly over the past decade. Initial studies largely focused on hand-crafted features and traditional machine learning methods to detect motor signs indicative of seizures. These approaches included the analysis of motion strength, motion trajectory, and differential luminance signals. While these methods achieved some success, their performance was often limited by changing luminance conditions or occlusions, such as a patient being covered by a blanket.

2.1 Model-Based Approaches

Karayiannis *et al.* [15, 16] explored computerized motion analysis of neonatal seizures using motion segmentation and tracking methods. These early efforts demonstrated the feasibility of automated seizure detection but highlighted challenges in generalizing across different settings and patient conditions. Ntonfo *et al.* [25] and Pisani *et al.* [26] further advanced these techniques by implementing low-complexity image processing algorithms for real-time detection of neonatal clonic seizures, achieving varying degrees of sensitivity and specificity.

Kalitzin *et al.* [14] focused on the automatic segmentation of episodes containing epileptic clonic seizures in video sequences. This study underscored the difficulty of maintaining performance in the presence of occlusions and varying illumination, common in clinical settings.

2.2 Deep Learning-Based Methods

Deep learning approaches have shown promise in overcoming the limitations of traditional methods. Ahmedt-Aristizabal *et al.* [4–6] and Achilles *et al.* [3] utilized deep neural networks for seizure detection, leveraging the ability of these models to learn spatio-temporal features directly from raw video data. These studies reported significant improvements in detection accuracy and robustness. However, deep learning methods often require large annotated datasets and substantial computational resources, which may not be readily available in many clinical settings.

Yang *et al.* [32] specifically addressed the detection of generalized tonic-clonic seizures using a combination of CNNs and long short-term memory (LSTM) networks. This study demonstrated that deep learning models could achieve high sensitivity (0.88) and specificity (0.92), outperforming earlier hand-crafted feature-based methods. Despite these promising results, the reliance on large training datasets and computational intensity remain significant limitations, particularly for real-time applications and environments with limited data availability.

2.3 Current Study

In our current study, we extend the body of work on video-based seizure detection by implementing a simple yet effective rule-based method for detecting clonic seizures. Our method leverages features including clinically relevant observations such as decreasing frequency of movement during a seizure. It also offers advantages in terms of computational efficiency and does not require extensive annotated datasets. As shown later, we implemented a smartphone-based app for the real-time detection. Our results indicate that with carefully

selected features and thresholds, our method can outperform more complex models within, at least, a controlled hospital setting.

3 Method

3.1 Video Acquisition

This study utilized video recordings from long-term video-EEG monitoring conducted at the National Center Hospital of Neurology and Psychiatry (NCNP) in Japan. The protocol received approval from the Research Ethics Committee of NCNP¹, and written informed consent was obtained from each participant, ensuring adherence to ethical guidelines.

For our proposed method, we strategically mounted the monitoring camera on the ceiling to ensure a comprehensive view of the patient, as illustrated in Figure 1. The camera setup is designed to operate under varying light conditions. During periods of adequate room illumination, the camera uses visible (RGB) light, complemented by an infra-red cut filter. In scenarios of low illumination, typically at night, the infra-red cut filter is automatically switched to a clear filter. This adjustment enhances the camera’s sensitivity, enabling continuous monitoring of the patient in both daytime and nighttime environments.

Significantly, our approach utilizes grayscale pixel values for seizure detection, a method equally effective under both lighting conditions. This uniformity allows us to apply the same algorithm regardless of the time of day.

The video-EEG system employed in this study records and compresses videos in the Windows Media Video format. The videos are captured at a resolution of 320×240 pixels and a frame rate of 30 frames per second (fps). Given that our method does not necessitate direct visualization of the patient’s body, the use of thin blankets by patients was permitted, further ensuring their comfort without compromising the effectiveness of the seizure detection process.

3.2 Blocking Frames

This section elaborates on the detection algorithm, focusing on the initial preprocessing steps. First, we convert the video into grayscale using the following formula:

$$I_t(x, y) = 0.2989 \cdot R_t(x, y) + 0.5870 \cdot G_t(x, y) + 0.1140 \cdot B_t(x, y). \quad (1)$$

¹IRB/ethics board protocol number: A2026-139, date of approval: April 21, 2017.

Here, $I_t(x, y)$ represents the grayscale value, and $R_t(x, y)$, $G_t(x, y)$, and $B_t(x, y)$ are the RGB pixel values at coordinates (x, y) in the t th frame. This transformation is akin to converting RGB to the Y component in the YUV color encoding system. For subsequent steps, we utilize only the grayscale values $I_t(x, y)$.

Given that the grayscale image I_t may include noise due to camera specifications, lighting conditions, or compression artifacts, we employ a noise reduction strategy. To mitigate these effects, we partition I_t into smaller blocks of a predetermined size. We then calculate the average pixel values within these blocks. This not only helps in alleviating noise but also reduces computational complexity.

For the block sizes, let M and N denote the dimensions. The average pixel value in each block $Z_t(a, b)$ is computed as follows:

$$Z_t(a, b) = \frac{1}{MN} \sum_{x=N(b-1)+1}^{Nb} \sum_{y=M(a-1)+1}^{Ma} I_t(x, y). \quad (2)$$

In this formula, (a, b) represent the block coordinates. In our study, we determined through experimentation that the optimal number of blocks per frame is 40×40 , which corresponds to $M = 6$ and $N = 8$.

3.3 Calculating Temporal Differences

As part of the detection algorithm, we first preprocess the video by transforming it into grayscale and then dividing it into blocks. The average of each block, denoted as $Z_t(a, b)$, tends to exhibit high energy in low-frequency components. To accentuate the oscillatory behavior relevant for seizure detection, we compute the temporal difference between neighboring frames as follows:

$$s_t(a, b) = Z_t(a, b) - Z_{t-1}(a, b). \quad (3)$$

This formula yields a set of time-series signals, $\{s(a, b)\}_{a,b}$, reflecting the patient's body movement.

3.4 Frequency Analysis

To analyze these time-series signals, we apply the Short-Time Fourier Transform (STFT) to convert $s(a, b)$ into its amplitude spectrum. The amplitude spectrum at time t is given by:

$$F_t(a, b, \mu) = |\text{FFT}_w(\hat{s}_t(a, b), \mu)|, \quad (4)$$

where FFT_w represents the fast Fourier transform with a window length of w , μ is the frequency (Hz), and $\hat{s}_t(a, b) := [s_{t-w+1}(a, b), \dots, s_t(a, b)]$. In our study, we chose $w = 300$ frames (10 seconds) with an overlap of 299 frames.

3.5 Seizure Detection

An illustrative spectrogram for a video sequence containing a tonic-clonic seizure is presented in Figure 2. This spectrogram, from a single block, effectively captures the clonic seizure. Two notable features can be observed:

1. Amplitudes in the 1–6 Hz frequency range are significantly larger during the seizure compared to other frequencies.
2. The dominant frequency decreases over time.

To quantify the first feature, we compute a contrast measure $C(a, b, t)$ as follows:

$$C(a, b, t) = \frac{L_2(a, b, t) - L_1(a, b, t) - L_3(a, b, t)}{L_2(a, b, t) + L_1(a, b, t) + L_3(a, b, t)}, \quad (5)$$

where $L_k(a, b, t)$ ($k \in \{1, 2, 3\}$) are expressed as

$$L_1(a, b, t) = \max_{0 < \mu < 1} F_t(a, b, \mu), \quad (6)$$

$$L_2(a, b, t) = \max_{1 \leq \mu < 6} F_t(a, b, \mu), \quad (7)$$

$$L_3(a, b, t) = \max_{6 \leq \mu < 10} F_t(a, b, \mu). \quad (8)$$

$C(a, b, t)$ is a modification of the spectral contrast [14]. This measure falls between $-1 \leq C(a, b, t) \leq 1$, indicating the likelihood of clonic seizures by comparing the amplitude in the 1–6 Hz range against other frequencies. Note that $C(a, b, t) > 0$ if $L_2(a, b, t) > L_1(a, b, t) + L_3(a, b, t)$.

For the second feature, recognized by epileptologists, we calculate the average dominant frequencies over two halves of a specified period, verifying if there is a decrease over time.

$$\begin{aligned} \mu_1(a, b, t) &= \frac{1}{l/2} \sum_i \arg \max_{\mu} F_i(a, b, \mu) \\ &\text{s.t. } t - l < i \leq t - l/2, \end{aligned} \quad (9)$$

$$\begin{aligned} \mu_2(a, b, t) &= \frac{1}{l/2} \sum_i \arg \max_{\mu} F_i(a, b, \mu) \\ &\text{s.t. } t - l/2 < i \leq t, \end{aligned} \quad (10)$$

where l is a temporal period. In (9), μ_1 is the average dominant frequency in the first half of the identifying period, whereas μ_2 is that in the second half. When $\mu_1(a, b, t) > \mu_2(a, b, t)$ is satisfied, we consider the dominant frequency to be decreasing. In this paper, $l = 30$ (1 s) is used.

Based on these observations, we define the following detection rule: **Detection Rule A**

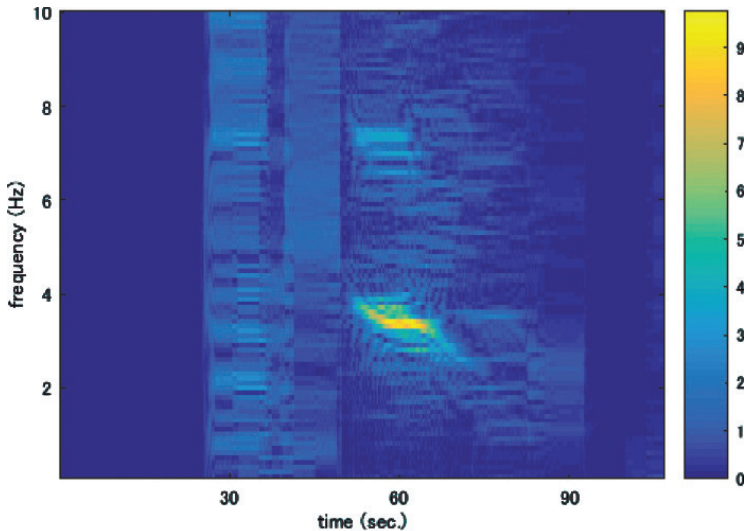


Figure 2: Spectrogram during epileptic seizure. This spectrogram is generated by (4). The horizontal axis represents time (s) and the vertical axis represents frequency. This includes focal seizure evolving to tonic-clonic seizure. The epileptic seizure begins at about 20 s The epileptic clonic seizure is at about 50–80 s.

A1 $C(a, b, t) > z_c$ persists for over 1 second.

A2 The average dominant frequency decreases during A1, i.e., $\mu_1(a, b, t) > \mu_2(a, b, t)$.

A3 The number of blocks satisfying A2 exceeds a threshold z_b .

These rules encapsulate the duration, frequency change, and widespread body oscillation characteristic of clonic seizures. The parameters z_b and z_c are optimized through cross-validation.

For comparison, we also explore Detection Rule B, which omits the frequency decrease criterion (A2). The efficacy of both detection rules (SDEC-A and SDEC-B) is assessed in an ablation study.

Note that Geertsema *et al.* [13] and Kalitzin *et al.* [14] only use the dominant frequency information as the “spectral footprint” of seizures. In contrast, our method uses the facts on the decrease of the dominant frequency.

4 Results and Discussion

This section outlines the experimental results of our proposed clonic seizure detection method.

Table 1: Video information. For seizure type, ‘‘F’’ and ‘‘TC’’ refer to focal seizure and tonic-clonic seizure, respectively.

Video	Patient	Sex	Age	Video length	Seizure type	Group
001	001	female	38	31 min 13 s	F, F → TC	A
002	002	female	30	39 min 45 s	F → TC	C
003_1	003	female	21	33 min 46 s	F → TC	A
003_2	003	female	21	15 min 11 s	F → TC	A
004	004	male	65	13 min 38 s	F → TC	C
005	005	female	43	30 min 1 s	F → TC	A
006	006	female	43	26 min 25 s	F → TC	C
007	007	male	47	44 min 57 s	F → TC	A
008	008	female	19	16 min 4 s	F → TC	B
009	009	female	24	48 min 32 s	F → TC	B
010_1	010	male	16	22 min 0 s	F → TC	B
010_2	010	male	16	9 min 41 s	F → TC	B
011_1	011	female	46	33 min 36 s	F → TC	C
011_2	011	female	46	42 min 36 s	F → TC	C
012	012	female	52	56 min 0 s	F → TC	B

4.1 Experimental Dataset

We used a dataset recorded at NCNP, comprising 15 tonic-clonic seizures from 12 epilepsy patients. Board-certified epileptologists performed the diagnosis and video segmentation. The total video length was 7 hours and 44 minutes, with specifications detailed in Section 3.1.

Table 1 summarizes the video and patient information, including cross-validation groupings. Notably, one video featured a focal seizure not evolving into a tonic-clonic seizure, treated as a non-seizure event for this study’s purposes.

4.2 Detection Accuracy Measures

We assessed performance using sensitivity and False Positive Length (FPL: seconds per 24 hours). Sensitivity is defined as

$$\text{Sensitivity} = \frac{n_{\text{TP}}}{n_{\text{TP}} + n_{\text{FN}}}, \quad (11)$$

where n_{TP} is the number of seizures detected during the seizure, and n_{FN} is the number of non-detected seizures. It is the ratio of detected seizures to the total number of seizures in the dataset.

Table 2: Detection Accuracy of Test Set.

SDEC-A					
Test set	Training set	z_b	z_c	Sensitivity	FPL (sec./24h)
A	B, C	60	0.06	0.8	0.0
B	A, C	50	0.06	1.0	0.0
C	A, B	40	0.10	1.0	0.0
Average		-		0.93	0.0
SDEC-B					
Test set	Training set	z_b	z_c	Sensitivity	FPL (sec./24h)
A	B, C	120	0.16	0.8	110.0
B	A, C	220	0.02	1.0	0.0
C	A, B	240	0.00	0.8	0.0
Average		-		0.87	36.7

FPL is defined as

$$\text{FPL (s/24h)} = \frac{\ell_{\text{FP}}}{\ell_{\text{FP}} + \ell_{\text{TN}}} \times 86400 \text{ (s/24h)}, \quad (12)$$

where ℓ_{FP} (s) is the total video length of false positives and ℓ_{TN} (s) is that of true negatives. It is calculated as the total length of false positives over the length of true negatives and non-seizure periods in the dataset. A 10-second blackout period was set post-seizure to accommodate the STFT’s 10-second window.

4.3 Detection Accuracy

We conducted three-fold cross-validation, dividing the dataset into groups with equal lengths and seizure counts. Parameters z_b and z_c were optimized from the training set, focusing on minimizing FPL while maintaining high sensitivity. Table 2 presents the experimental results, showing SDEC-A’s superior accuracy over SDEC-B, highlighting the importance of dominant frequency changes in seizure detection.

The robustness of the algorithm was also evaluated. Figures 3 and 4 compare parameter combinations for z_b and z_c , with the optimal combination indicated by a red “x”. The area surrounded by green lines shows the parameter combination of the sensitivity of 1 and FPL of 0, which validates the robustness of the proposed algorithm according to the parameter setting.

SDEC-A consistently achieved Sensitivity = 1 and FPL = 0 across all training sets, unlike SDEC-B. This variability in SDEC-B’s performance suggests a dataset sensitivity, further validating the robustness of SDEC-A’s approach. Note that some patients used blankets: This does not affect the overall performance.

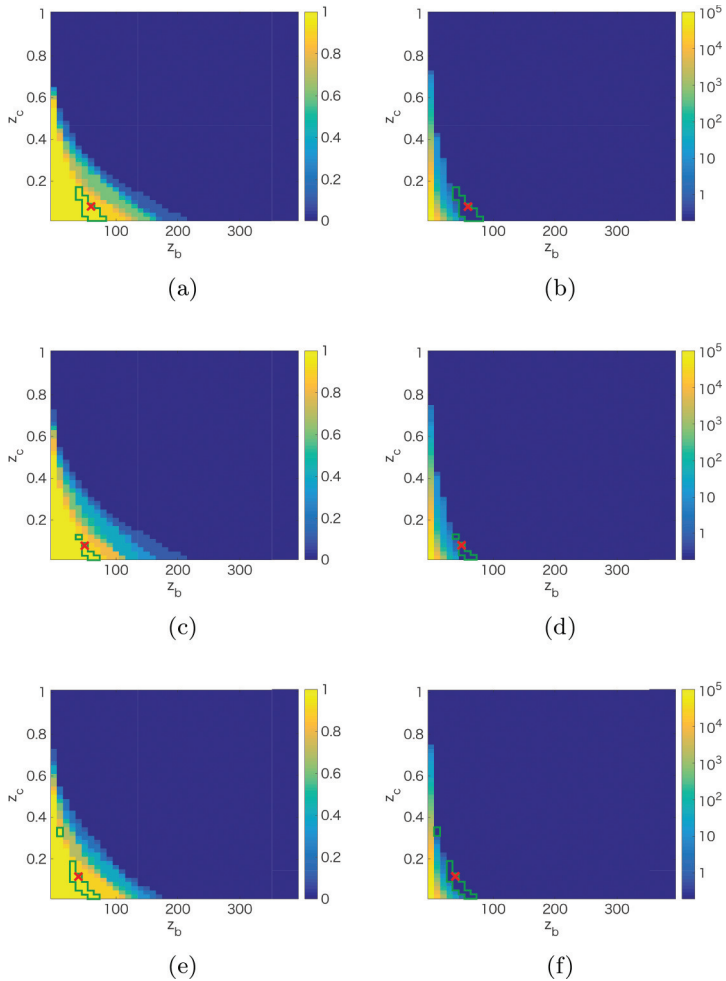


Figure 3: Detection accuracy according to parameter combination of z_b and z_c . We used SDEC-A and the accuracy for the training set is shown. (a) Sensitivity of B and C. (b) FPL of B and C. (c) Sensitivity of A and C. (d) FPL of A and C. (e) Sensitivity of A and B. (f) FPL of A and B.

We also determined the best parameter combination using the entire dataset, as shown in Table 3. Consistent with cross-validation findings, SDEC-A outperformed SDEC-B, achieving 100% detection accuracy.

While the dataset is not the same, the state-of-the-art deep learning-based method Yang *et al.* [32] presents the sensitivity 0.88. This implies the detection accuracy of our algorithm could be comparable to deep learning-based method

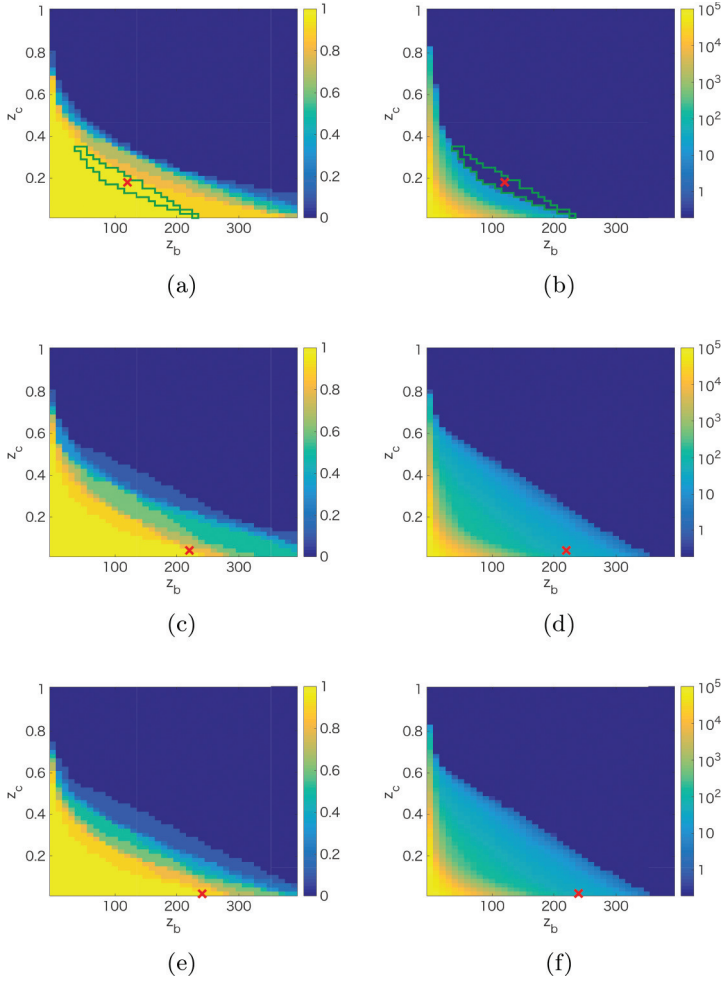


Figure 4: Detection accuracy according to parameter combination of z_b and z_c . We used SDEC-B and the accuracy for the training set is shown. (a) Sensitivity of B and C. (b) FPL of B and C. (c) Sensitivity of A and C. (d) FPL of A and C. (e) Sensitivity of A and B. (f) FPL of A and B.

with significantly fewer parameters. It is beneficial for real-time detection that is highly demanding for hospitals, homes, and many other places.

For SDEC-A, the latency after presumed clinical seizure onset is less than 12 seconds for all patients. This is significantly shorter than the result reported in the state-of-the-art deep learning-based method [32].

Table 3: Parameter Combination by Using All Data as Test Set.

	z_b	z_c	Sensitivity	FPL (sec./24h)
SDEC-A	50	0.04	1.0	0.0
SDEC-B	220	0.02	1.0	26.6



Figure 5: Prototype for a smatphone app.

4.4 Computation Time

Our experiments, conducted on MATLAB R2016b with a 3.6 GHz Intel Core i7-6950X processor and 32 GB RAM, assessed both offline and online processing times.

4.4.1 Offline Processing

For offline video processing, SDEC-A and SDEC-B averaged 109 and 110 fps, respectively. This indicates that the dominant frequency change condition does not significantly impact computation time, suggesting the method's feasibility for rapid video-EEG analysis.

4.4.2 Online Processing

We implemented a GUI for real-time processing from webcams at 320×240 resolution and 30 fps. The experiment confirmed real-time processing capability at 30 fps for both SDEC-A and -B. Given the method's focus on 0–10 Hz frequency components, a camera frame rate of 20 fps would suffice, further reducing computational requirements.

Additionally, we developed a prototype utilizing a Google Pixel 6 Pro smartphone and a standard surveillance web camera (ELP USBFHD05MT-

DL36), as depicted in Figure 5. This prototype is capable of functioning in real-time during both daytime and nighttime conditions.

5 Conclusion and Future Research

This paper introduces a simple yet effective method for video-based epileptic seizure detection. Our approach, requiring only a ceiling-mounted video camera, focuses on analyzing temporal pixel value changes and detecting dominant frequencies in the 1–6 Hz range. The method also leverages the clinical observation of decreasing dominant frequencies during clonic seizures. Experiments with 15 tonic-clonic seizures from 12 patients demonstrated high detection accuracy and real-time processing capability on standard computers. Future research will aim to develop an efficient method for selecting optimal parameter combinations. Because the video-EEG monitoring system we used only recorded the data (including videos) during seizures, we do not have any videos without seizures. Future work also includes the extensive studies for longer monitoring periods and experiments beyond video-EEG monitoring using our prototype.

References

- [1] E. Acar, C. Aykut-Bingol, H. Bingol, R. Bro, and B. Yener, “Multiway analysis of epilepsy tensors”, *Bioinformatics*, 23(13), 2007, i10–i18.
- [2] E. Acar, C. A. Bingol, H. Bingol, R. Bro, and B. Yener, “Seizure recognition on epilepsy feature tensor”, in *Prop. Int. Conf. IEEE Eng. Med. Biol. Soc.* 2007, 4273–6.
- [3] F. Achilles, F. Tombari, V. Belagiannis, A. M. Loesch, S. Noachtar, and N. Navab, “Convolutional neural networks for real-time epileptic seizure detection”, *Computer Methods in Biomechanics and Biomedical Engineering: Imaging & Visualization*, 6(3), 2018, 264–9.
- [4] D. Ahmedt-Aristizabal, C. Fookes, S. Denman, K. Nguyen, S. Sridharan, and S. Dionisio, “Aberrant epileptic seizure identification: A computer vision perspective”, *Seizure*, 65, 2019, 65–71.
- [5] D. Ahmedt-Aristizabal, C. Fookes, S. Dionisio, K. Nguyen, J. P. S. Cunha, and S. Sridharan, “Automated analysis of seizure semiology and brain electrical activity in presurgery evaluation of epilepsy: A focused survey”, *Epilepsia*, 58(11), 2017, 1817–31.
- [6] D. Ahmedt-Aristizabal, C. Fookes, K. Nguyen, S. Denman, S. Sridharan, and S. Dionisio, “Deep facial analysis: A new phase I epilepsy evaluation using computer vision”, *Epilepsy & Behavior*, 82, 2018, 17–24.

- [7] B. Blankertz, R. Tomioka, S. Lemm, M. Kawanabe, and K.-R. Muller, "Optimizing spatial filters for robust EEG single-trial analysis", *IEEE Signal Process. Mag.*, 25(1), 2008, 41–56.
- [8] G. T. Borujeny, M. Yazdi, A. Keshavarz-Haddad, and A. R. Borujeny, "Detection of epileptic seizure using wireless sensor networks", *J. Med. Signals Sens.*, 3(2), 2013, 63.
- [9] D. Cogan, M. Nourani, J. Harvey, and V. Nagaraddi, "Epileptic seizure detection using wristworn biosensors", in *Prop. Int. Conf. IEEE Eng. Med. Biol. Soc.* 2015, 5086–9.
- [10] I. Conradsen, S. Beniczky, P. Wolf, P. Jennum, and H. B. Sorensen, "Evaluation of novel algorithm embedded in a wearable sEMG device for seizure detection", in *Prop. Int. Conf. IEEE Eng. Med. Biol. Soc.* 2012, 2048–51.
- [11] K. Cuppens, L. Lagae, B. Ceulemans, S. Van Huffel, and B. Vanrumste, "Automatic video detection of body movement during sleep based on optical flow in pediatric patients with epilepsy", *Med. Biol. Eng. Comput.*, 48(9), 2010, 923–31.
- [12] A. B. Gardner, A. M. Krieger, G. Vachtsevanos, and B. Litt, "One-class novelty detection for seizure analysis from intracranial EEG", *J. Mach. Learn. Res.*, 7(Jun), 2006, 1025–44.
- [13] E. E. Geertsema, R. D. Thijs, T. Gutter, B. Vledder, J. B. Arends, F. S. Leijten, G. H. Visser, and S. N. Kalitzin, "Automated video-based detection of nocturnal convulsive seizures in a residential care setting", *Epilepsia*, 59, 2018, 53–60.
- [14] S. Kalitzin, G. Petkov, D. Velis, B. Vledder, and F. L. da Silva, "Automatic segmentation of episodes containing epileptic clonic seizures in video sequences", *IEEE Trans. Biomed. Eng.*, 59(12), 2012, 3379–85.
- [15] N. B. Karayiannis, G. Tao, J. D. Frost, M. S. Wise, R. A. Hrachovy, and E. M. Mizrahi, "Automated detection of videotaped neonatal seizures based on motion segmentation methods", *Clin. Neurophysiol.*, 117(7), 2006, 1585–94.
- [16] N. B. Karayiannis, G. Tao, Y. Xiong, A. Sami, B. Varughese, J. D. Frost, M. S. Wise, and E. M. Mizrahi, "Computerized motion analysis of videotaped neonatal seizures of epileptic origin", *Epilepsia*, 46(6), 2005, 901–17.
- [17] N. B. Karayiannis, Y. Xiong, G. Tao, J. D. Frost, M. S. Wise, R. A. Hrachovy, and E. M. Mizrahi, "Automated detection of videotaped neonatal seizures of epileptic origin", *Epilepsia*, 47(6), 2006, 966–80.
- [18] U. Kramer, S. Kipervasser, A. Shlitner, and R. Kuzniecky, "A novel portable seizure detection alarm system: preliminary results", *J. Clin. Neurophysiol.*, 28(1), 2011, 36–8.

- [19] S. N. Larsen, I. Conradsen, S. Beniczky, and H. B. Sorensen, "Detection of tonic epileptic seizures based on surface electromyography", in *Prop. Int. Conf. IEEE Eng. Med. Biol. Soc.* 2014, 942–5.
- [20] Z. Li, A. M. da Silva, and J. P. S. Cunha, "Movement quantification in epileptic seizures: a new approach to video-EEG analysis", *IEEE Trans. Biomed. Eng.*, 49(6), 2002, 565–73.
- [21] H. Lu, H.-L. Eng, C. Guan, K. N. Plataniotis, and A. N. Venetsanopoulos, "Regularized common spatial pattern with aggregation for EEG classification in small-sample setting", *IEEE Trans. Biomed. Eng.*, 57(12), 2010, 2936–46.
- [22] H. Lu, Y. Pan, B. Mandal, H.-L. Eng, C. Guan, and D. W. Chan, "Quantifying limb movements in epileptic seizures through color-based video analysis", *IEEE Trans. Biomed. Eng.*, 60(2), 2013, 461–9.
- [23] F. Massé, J. Penders, A. Serteyn, M. van Bussel, and J. Arends, "Miniaturized wireless ECG-monitor for real-time detection of epileptic seizures", in *Proc. Wireless Health*, 2010, 111–7.
- [24] T. M. Nijssen, J. B. Arends, P. A. Griep, and P. J. Cluitmans, "The potential value of three-dimensional accelerometry for detection of motor seizures in severe epilepsy", *Epilepsy Behav.*, 7(1), 2005, 74–84.
- [25] G. M. K. Ntonfo, G. Ferrari, R. Raheli, and F. Pisani, "Low-complexity image processing for real-time detection of neonatal clonic seizures", *IEEE Transactions on Information Technology in Biomedicine*, 16(3), 2012, 375–82.
- [26] F. Pisani, C. Spagnoli, E. Pavlidis, C. Facini, G. M. K. Ntonfo, G. Ferrari, and R. Raheli, "Real-time automated detection of clonic seizures in newborns", *Clinical neurophysiology*, 125(8), 2014, 1533–40.
- [27] E. Schulc, I. Unterberger, S. Saboor, J. Hilbe, M. Ertl, E. Ammenwerth, E. Trinka, and C. Them, "Measurement and quantification of generalized tonic-clonic seizures in epilepsy patients by means of accelerometry—an explorative study", *Epilepsy Res.*, 95(1-2), 2011, 173–83.
- [28] A. Shoeb, H. Edwards, J. Connolly, B. Bourgeois, S. T. Treves, and J. Guttag, "Patient-specific seizure onset detection", *Epilepsy Behav.*, 5(4), 2004, 483–98.
- [29] C. Á. Szabó, L. C. Morgan, K. M. Karkar, L. D. Leary, O. V. Lie, M. Girouard, and J. E. Cavazos, "Electromyography-based seizure detector: Preliminary results comparing a generalized tonic-clonic seizure detection algorithm to video-EEG recordings", *Epilepsia*, 56(9), 2015, 1432–7.
- [30] D. J. Thurman, E. Beghi, C. E. Begley, A. T. Berg, J. R. Buchhalter, D. Ding, D. C. Hesdorffer, W. A. Hauser, L. Kazis, R. Kobau, B. Kroner, D. Labiner, K. Liow, G. Logroscino, M. T. Medina, C. R. Newton, K. Parko, A. Paschal, P. Preux, J. W. Sander, A. Selassie, W. Theodore, T. Tomson, and S. Wiebe, "Standards for epidemiologic studies and surveillance of epilepsy", *Epilepsia*, 52, 2011, 2–26.

- [31] W. J. Van Elmpt, T. M. Nijsen, P. A. Griep, and J. B. Arends, “A model of heart rate changes to detect seizures in severe epilepsy”, *Seizure*, 15(6), 2006, 366–75.
- [32] Y. Yang, R. A. Sarkis, R. El Atrache, T. Loddenkemper, and C. Meisel, “Video-based detection of generalized tonic-clonic seizures using deep learning”, *IEEE Journal of Biomedical and Health Informatics*, 25(8), 2021, 2997–3008.